ГЛАСНИК Српског географског друштва 106(1) 539-566
BULLETIN OF THE SERBIAN GEOGRAPHICAL SOCIETY 2026

Original scientific paper UDC 556.388(65)
https://doi.org/10.2298/GSGD2601539B

Received: October 23, 2025
Corrected: March 9, 2026
Accepted: May 8, 2026

Mohamed hicham Boutelli[1]*,, Tahar Selmane**, ***, Hafidha Khebizi****, Senna Lachehab**, Lakhdar Seraiche***, Mostefa Dougha*****

**Laboratory of oil, gas and water aquifers, Faculty of Hydrocarbons, Renewable Energies and Earth and Universe Sciences, Kasdi Merbah-Ouargla University, Algeria*
*** Department of Hydraulics and Civil Engineering, Faculty of Science and Technology University of Ghardaia, Algeria*
**** VEHDD Laboratory, faculty of technology, University of M'sila, M'sila, Algeria*
***** MVRE Laboratory, the National Higher School of Hydraulics, Blida, Algeria*

ASSESSMENT OF GROUNDWATER NITRATE CONTAMINATION AND ITS ORIGIN IN THE BOUSAADA REGION, ALGERIA

Abstract: Groundwater is the principal water resource in the semi-arid region of Bousaada. This study assesses hydrochemical characteristics, temporal evolution, and sources of nitrate contamination using more than 200 groundwater samples, including current sampling and archived dataset. Groundwater is characterized by the dominance of Cl^- and SO_4^{2-}, together with Ca^{2+} and Mg^{2+}, indicating contributions from evaporitic dissolution and carbonate processes. Most samples exceeded guideline values for of NO_3^-, and a large proportion surpassed chloride and sulfate standards. Temporal analysis (1967–2022) reveals a sustained increase in nitrate concentrations, with mean values reaching about 128 mg/L, and 50% of newly analysed samples exceeded 100 mg/L. Pollution indices and health risk assessment indicate that the majority of groundwater samples are highly contaminated and pose significant health risks, particularly in agricultural zones and near Wadi Bousaada. Hydrochemical ionic ratios, and multivariate (PCA) analysis, indicate that nitrate contamination primarily originates from agricultural fertilizers and septic tank effluents, with additional influence from Wadi Bousaada. Spatial modeling using kriging approaches improved prediction accuracy and highlighted hotspots in the Maadher agricultural area and near Wadi Bousaada. The findings demonstrate significant groundwater quality deterioration over five decades and emphasize the urgent need for improved agricultural and sanitation management.

Keywords: nitrate pollution, groundwater, Bousaada, Kriging, health risk, semi-arid region

[1] boutelli.mohamed.hicham@univ-ghardaia.edu.dz(corresponding author)
Tahar Selmane (https://orcid.org/0000-0001-6233-6536)
Senna Lachehab (https://orcid.org/0000-0002-7701-9928)
Lakhdar Seraiche (https://orcid.org/0000-0002-0652-5663)
Mostafa Dougha (https://orcid.org/0000-0001-9776-1321)

Introduction

The daily essential water needs of millions of people, whether for drinking, agriculture, or industry, are primarily dependent on groundwater. However, with the fast increase of population and the expansion of agricultural and industrial activities, groundwater is increasingly and severely exposed to various sources of pollution that threaten its quality and pose significant risks to public health.

Nitrate is a common soluble contaminant of groundwater (Li et al., 2021a, 2021b) and readily accumulates, with the main drivers of high nitrate concentrations being anthropogenic activities, such as the release of domestic and industrial wastewater into the environment and agricultural activities (Roy et al., 2007; Stelzer et al., 2011; Wu et al., 2019). Since elevated nitrate contributes to eutrophication of water resources, nitrate pollution is a serious problem affecting regional groundwater quality. Groundwater at a global level is currently under threat by nitrate contamination to varying degrees (Rahmati et al., 2015; Wu et al., 2019). The long-term consumption of groundwater containing excessively high nitrate can pose a risk to human health, leading to diseases such as methemoglobinemia (Shams et al., 2009), cancer of various organs of the digestive system (Anjana & Iqbal, 2007), and blue baby syndrome (Xin et al., 2021). Although groundwater nitrate concentrations are within the World Health Organization (WHO) drinking water standard of 50 mg/L, they remain a non-carcinogenic health risk to humans, and particularly to children and infants (Kamarehie et al., 2019; Qasemi et al., 2020). An understanding of the nitrate content of groundwater and the associated human health risks (Azhdarpoor et al., 2019; Radfard et al., 2019; Yousefi et al., 2018) can assist decision makers in developing water resource protection measures.

This study focuses on assessing groundwater quality, evaluating nitrate pollution in Bousaada, located in Hodna region, a semi-arid area in northeast of Algiers and identifying the origin of nitrate contamination. Furthermore, the research examines the role of physical factors in exacerbating groundwater nitrate pollution. By employing methodologies such as statistical analyses, nitrate pollution index (NPI), human health risk assessment (HHRA), and advanced spatial modeling techniques like co-kriging, this study aims to provide a comprehensive understanding of the issue and contribute to sustainable water resource management.

General setting

Location and human activities

Bousaada is located in Hodna, northeast of Algiers. It is situated between longitudes 4°21' E to 4°32' E and latitudes 35°24' N to 35°34' N. Bousaada region is covered by sandy material and shows a variety topography, which, according to Fig. 1, is thought to regulate how the streams drain (Selmane et al., 2022b).

In the study area of Bousaada there is a significant agricultural region thanks to the sandy loam soil that is suitable for cultivation. Pumping for irrigation from the water table can be anywhere between 30 and 120 meters deep, where the majority of wells do not conform to the equipment and insulation requirements of subpar aquifers. Agricultural land includes agricultural facilities, and is used to cultivate and harvest crops for human and animal consumption as well as grazing.

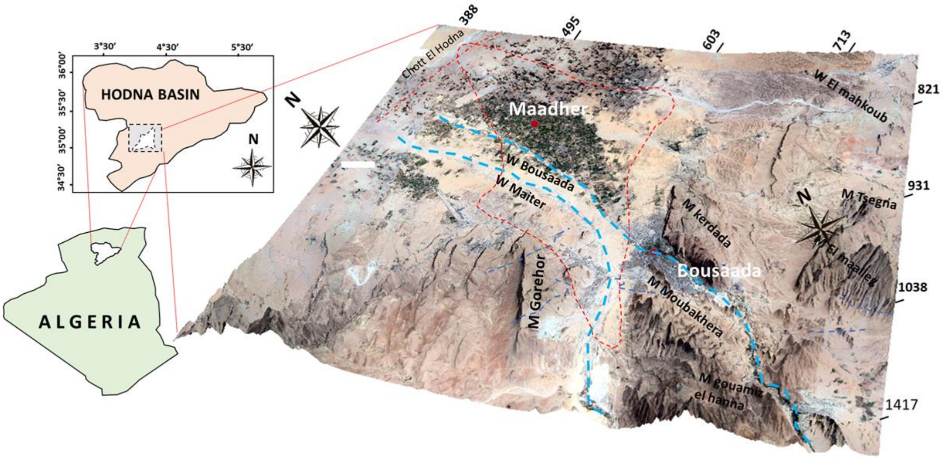

Fig. 1. Location map of the Bousaada region

Climate Geology and Hydrogeology

Bousaada climate is a part of the Hodna Mediterranean climate that has a tendency to aridity (Kebiche, 1998). It shows two distinct seasons: the first is a hot and dry summer while the second is a humid winter. The yearly precipitation ranges from 250 to 300 mm in Maarif, Khoubana and Ouled Sidi Brahim (Kebiche, 1998; Boudjemline, 2018) from 175 to 200 mm going toward Chott and from 250 to 300 mm going toward Bousaada (Kebiche, 1998). The rainfall distribution is related to geomorphology and becomes more important in areas that have elevation exceeding 400 m above the sea level notably in Boussaada municipality (Kebiche, 1998). In addition, a poorly distributed rainfall is observed throughout the year, with a mean monthly temperature of 22°C (Boudjemline, 2018).

From a geological point of view, the Maadher is in a closed foredeep basin whose filling sequence begins with continental deposits of Eocene and Oligocene and continues with a Miocene (Askri et al., 1995). This basin is at an altitude of 400 m where Hodna Chott going to the north forms the basin's bottom (Kebiche, 1998). The basin is part of the Hodna watershed that marks the transition between the Tell domain to the north and the Sahara to the south. The passage between these two domains is shown by a succession of mountain ranges and plains that allow the diversity of bioclimatic environments (Kebiche, 1998).

The geological map (Figure 2) shows a Triassic and Cretaceous sedimentary formations that outcrop in the western and the southern part of the Maadher. The Miocene appears in the south while the center and the east and the north are covered by Quaternary, recent dune, and alluvial material. The detrital material notably conglomerates are found at various levels, especially at the base of the Neogene, and at the top of the Pliocene, where their maximum thickness is 600 m (Maurice et Jean, 1977). At the Hodna scale, the geomorphology indicates the existence of "barrier reliefs" blocking the migration of sands from Hodna and "corridor reliefs" facilitating the transfer of sands. In this vast transatlas flow, hydrowind depressions seem to maintain the permanence of the phenomenon (Benazzouz, 1994).

From a hydrogeological point of view, the Maadher receives the flow from the surface and underground waters. The runoff quickly turns into floods, which are spectacular and sometimes even disastrous (Kebiche, 1998). The principal aquifers in the study region are the conglomerate and sandy Mio-Pliocene, which are connected to Cretaceous sandy formations, the upper Albian being the most important (Askri, 1995; Guiraud, 1970; 1973).

Rainfall through the wadis and irrigation water are the main sources of groundwater recharge. The sandy water table of Quaternary and Mio-pliocene age are connected to old groundwater thanks to brittle deformation, which allows Cretaceous terrain to come into outcrop (Abdesselam et al., 2013). The groundwater from Quaternary aquifer is relatively salinized.

In the middle of the plain, the Mio-Plio-Quaternary aquifer has a thickness of more than 250 m. (Guiraud, 1973; Derekov, 1973). The study area's stratigraphy includes a variety of alternations, frequently disorganized, of sandy clays, clays, sandstones, or occasionally clayey sands and conglomerates at the top.

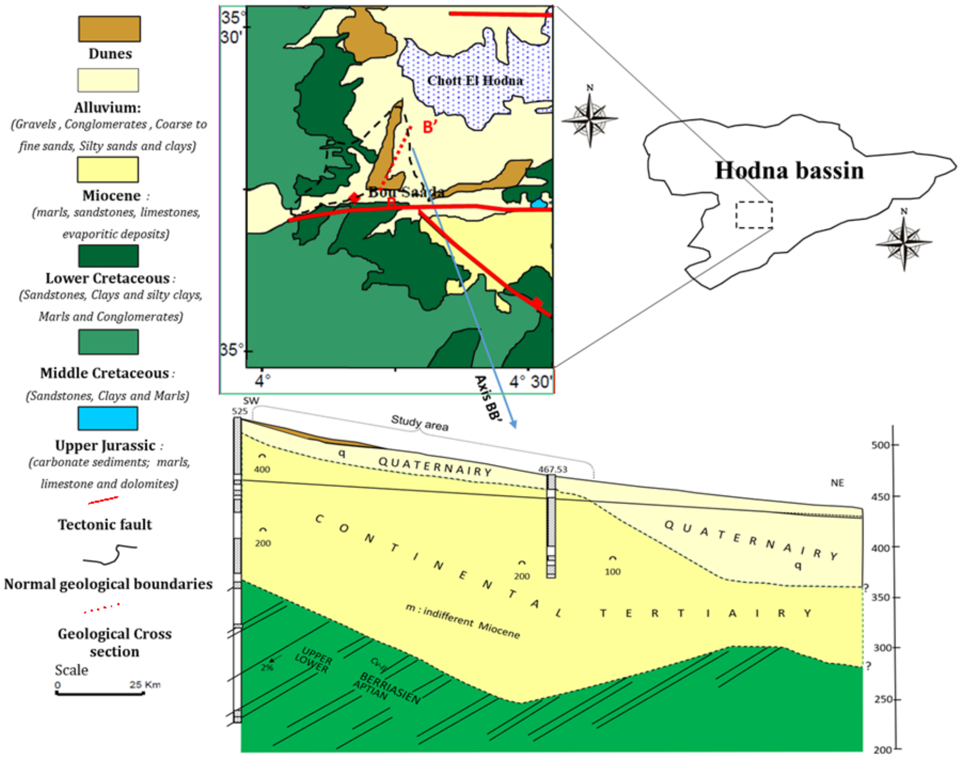

Fig. 2. Geological map of Bousaada region in the Hodna Basin, highlighting the geological section along the axis B-B'.

Pedology

Soil is an important natural source, which ensures the permanent production of the nutrients necessary for the life of human beings. Minerals, organic matter, water, and air form soil where dominance percentage is respectively 45%, 5%, 30% and 30%. Generally, soil chemical composition depends on parent rock (Benchetrif, 1956). In Hodna, the originality of the pedogenesis processes that depends on a mixed climate: humid temperate with arid affinities, makes the soil classification different from that defined in Europe (Benchetrif, 1956). According to the pedological map of Hodna (Bayadgifv, 1975), Hodna

Chott is formed by allomorphic, hydromorphic and aeolian raw minerals soils. Going to the north a saline area is developed forming little evolved alluvial soils. On the periphery calcareous crusts, lithosols and Sierozems dominate. While going towaed the south of Hodna Chott, the following soil zonation is determined: a halomorphic soil and raw aeolian mineral soils; salty hydromorphic soil and raw aeolian mineral soils; raw aeolian mineral soils with pockets of lithosol and rigosol and poorly evolved alluvial soils; lithosol and calcalerous crusted and gypsum soil (show Figure 3).

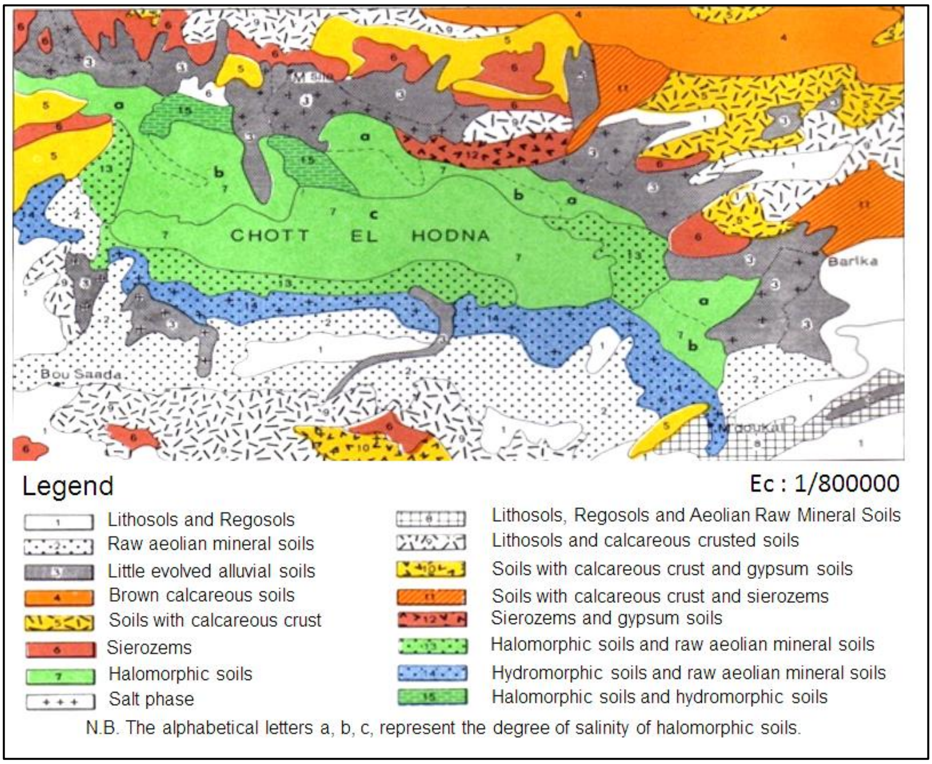

Fig. 3. Pedology map of Hodna (Boyadgifv, 1975)

Land use

Generally, the Hodna is a very impoverished steppe. It is to the climate that we must finally attribute the abundance of fertilizing elements in the sufficiently light soils of the middle part of the plain, but also the high salinity of many of the lower heavy soils and the general poverty of all soils in humus. Hodna has produced cereals at various times.

The study area benefits from a vast irrigated plain located northeast of the city of Bousaada. There are, according to the department of the agricultural services of Bousaada (DSA), approximately 42000 hectares of arable land, 50% of which are irrigated (Abdesselam et al., 2012). Maadher is the area with the greatest agricultural activity, the lands of this city are estimated to be very good for agriculture, with more than 2595 hectares, of which 2299 are irrigated, or 88.6% of the total cultivated area. The Maadher plain has become a major agricultural area irrigated by pumping groundwater since the 1970s. Crops can be grown on its brown and reddish-brown sandy clay soils. Synthetic fertilizers and animal waste are usually applied frequently (once every two years).

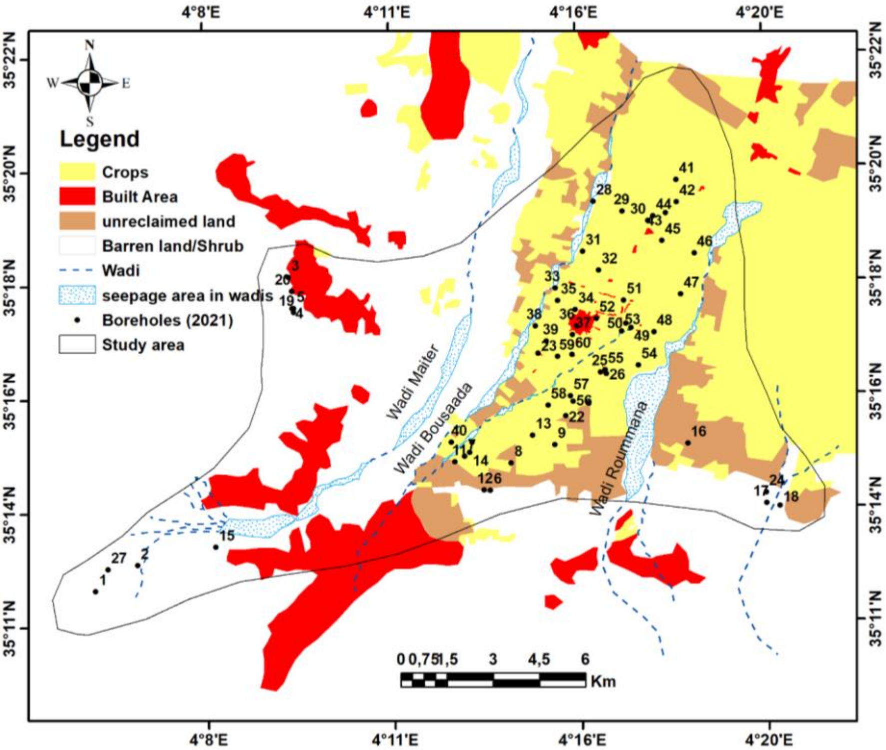

Fig. 4. Land use map of Bousaada region

Soil microbial activity

The complexity and the biological dynamism of soil make it difficult to define the microbial communities in soil (Nannipieri et al., 2003). The land use and the soil types significantly influence microbial activity (Gangwar et al., 2022), which indicates the metabolic processes, notably CO_2 evolution, nitrification, and denitrification rate, the incorporation of thymidine, and dehydrogenase activity etc. (Nannipieri et al., 2003). The nitrifier and denitrifier communities react to saline and alkaline stress conditions that increase the pH of the soil, where the abundance, diversity, and structure are affected (Guo et al., 2021). In addition, the enrichment in nitrogen elements leads to ecosystem dysfunction and the disruption of communities, leading to the development of pathogenic microorganisms (Park et al., 2020), which make water unsuitable.

In Southern Hodna, a rupture with traditional land used for pastoralism is observed due to the extension of irrigated agriculture and overpumping from groundwater (Abdesselam, 2012). Consequently, nitrate contamination affected the water table (Abdesselam, 2012), but the use of septic tanks by the population of Maadher (Selmane, 2023) also amplified the water nitrate pollution. The nitrification process is influenced by soil salinity, which disturbs the normal pathway of N transformations and inhibits the nitrification's second step, producing the accumulation of nitrite in soil (Akhtar et al., 2012).

Material and Methods

The methodology of this research project consists of four main phases: collecting the data and laboratory analysis, verification of groundwater quality, evaluation of nitrate pollution in the study area, and proving the origin of groundwater pollution with nitrates. The flowchart in Figure 5 illustrates the methodology used for the study in detail.

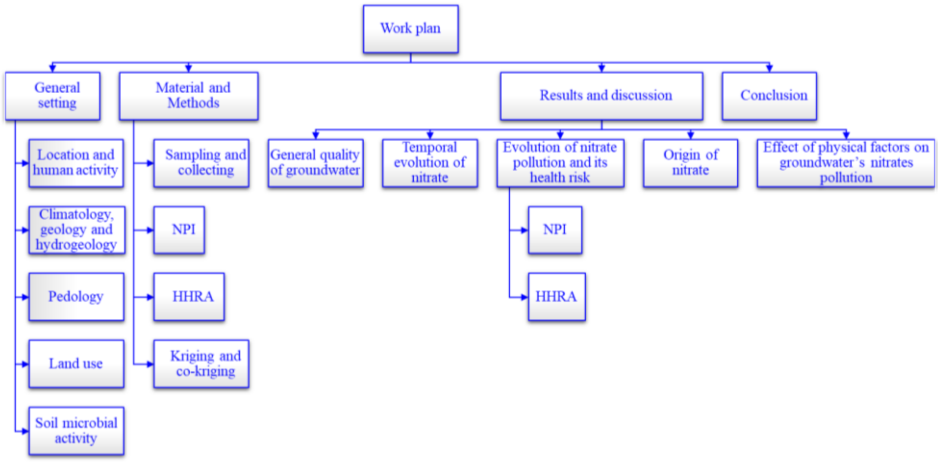

Fig. 5. Flowchart displaying the methodology followed

Sampling and collecting

This study used physico-chemical data from 219 samples, divided into two types: archived data for 159 samples from 1967, 1996, 2018, and 2019, and recent data for 60 samples collected between November 17 and 20, 2022.

Regarding the recent data, the selected boreholes are used for drinking, irrigation, and other daily purposes. Selection took into account boreholes located near population centers (Maadher), Wadi Maiter, Wadi Bousaada, and boreholes located within agricultural areas (Fig 4). The depth of these boreholes ranges between 100 and 200 meters. The samples were collected using the conventional sampling protocol (Wilde, 2010). The samples collected were put in polyethylene bottles. The pH, temperature, and electrical conductivity (EC) were all measured at the site using WTW 3110. Concentrations of Na^+, K^+ were determined using Agilent 200 series U systems. Sulfate, ammonium, nitrite and nitrate were measured by the colorimetric method with the Odyssey DR/2500 spectrophotometer. While Ca^{2+}, Mg^{2+}, HCO_3^- and Cl^- were analyzed by volumetric titration. For each parameter analysis, the measurement is repeated twice.

For the archived data, a set of physicochemical parameters (pH, EC, TDS, Ca^{2+}, Mg^{2+}, Na^+, K^+, Cl^-, SO_4^{2-}, HCO_3^-, NO_3^- and NO_2) of boreholes in the Bousaada region was used to study the evolution of nitrates concentrations. The dataset included 61 water points surveyed by FAO in 1967, 50 water points by ANRH in 1996, and 19 and 29 water points by ADE in 2018 and 2019 respectively. It should be noted that the samples from the 1967 and 1996 campaigns are taken from the water table with an average depth of less than 50 m (Derekov, 1973).

To ensure consistency between archived datasets and newly collected samples and to procedure an accurate comparison, only physicochemical parameters that were consistently reported in both the historical datasets and the current sampling campaign were considered in the analysis. The analytical methods used in the archived sources were reviewed and found to be comparable with the standard hydro chemical analytical techniques applied in the recent study. Samples with incomplete records or anomalous values were excluded. In addition, the ionic balance error was checked to confirm the internal consistency of the hydro chemical data.

Principal component analysis

Principal Component Analysis (PCA) is a multivariate statistical technique. It is used to reduce the number of variables without sacrificing too much information, also it allows for the exploration of correlations between variables and similarities between individuals (Selmane et al., 2002b). PCA was applied to identify the main hydrogeochemical processes controlling groundwater quality in Bousaada and to reduce dataset dimensionality. The analysis included standardized physicochemical parameters from the November 2022 campaign (60 samples): pH, EC, TDS, TH, Ca^{2+}, Mg^{2+}, Na^{+}, K^{+}, HCO_3^{-}, Cl^{-}, SO_4^{2-}, and NO_3^{-}. The Kaiser criterion (Kaiser, 1960) was applied to determine the total number of significant principal components. According to this criterion, only the principal components whose eigenvalue is greater than or equal to 1 have been retained as a possible source of variance in the data.

Nitrate Pollution Index (NPI)

Nitrate contamination of groundwater and its effects on human health is one of the most important life-threatening issues that are monitored worldwide (Panneerselvam et al., 2020). The NPI application is an indicator used to assess the level of nitrate pollution in groundwater due to human activity (Bahrami et al., 2020). When the concentration of NO_3^{-} in groundwater exceeds 20 mg/l, it can be considered as anthropogenic pollution (Reddy et al., 2022). The maximum permissible level of NO_3^{-} in drinking water is 50 mg/l (WHO, 2011). Nitrate pollution of groundwater has been monitored using NPI index in many parts of the world, as this indicator gives a clear picture of the percentage of water pollution (Panneerselvam et al., 2021; Reddy et al. 2022; Bahrami et al., 2020; Obeidat et al., 2012; El Mountassir et al., 2022). The following equation was applied to calculate NPI

$$NPI = \frac{(C_s - HAV)}{HAV} \quad (1)$$

where: Cs represents the analytical range of nitrate in the water sample; HAV represents the threshold value of the artificial source (20 mg/l).

According to the NPI value, the water quality is divided into five categories: Very good (< 0) (no pollution), good (0 to 1) (slightly polluted), moderate status (1 to 2) (moderately polluted), poor status (2 to 3) (heavily polluted) and bad status (> 3) (very heavily polluted).

Human Health Risk Assessment (HHRA)

The United States Environmental Protection Agency (USEPA) proposed the human health risk evaluation model as a method of assessment that sheds light on the effects of consuming highly Contaminated groundwater's implications on health (Panneerselvam et al., 2021; Adimalla et al., 2020).

Different contaminants enter the body of humans in various ways, but drinking water is probably the most significant. Risks from carcinogens and non-carcinogens are the two categories under which the effects are categorized (Panneerselvam et al., 2021). The HHRA is divided into four stages: risk identification in stage 1, assessment in stage 2, exposure in stage 3, and hazard characterization in stage 4 (Reddy et al., 2022). To evaluate non-carcinogenic risks, three age groups of people children, men, and women have been taken into consideration (Adimalla et al., 2018). By ingesting drinking water and coming into contact with skin, it risks are deemed non-carcinogenic (Zhang et al., 2018).

Nitrate was selected to assess the non-carcinogenic risk in this study due to its high concentrations in groundwater samples, while the concentration of other non-carcinogenic parameters is very low. The drinking water was considered in this study, as it is the primary pathway of human exposure to NO_3^- in groundwater, while other exposure pathways are negligible. This study also considered children and adults to reflect the effects of groundwater NO_3^-. It is possible to calculate the HHRA model through water intake as illustrated in Figure 6 (Xu et al., 2023):

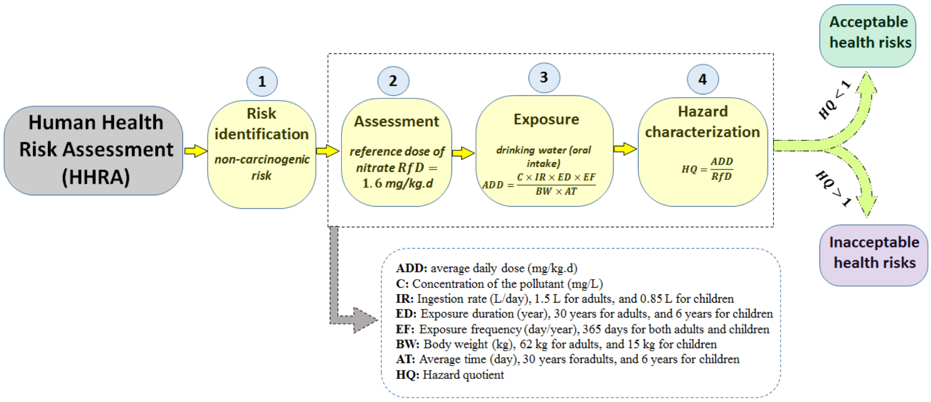

Fig. 6. Flowchart Procedures of non-carcinogenic health risk assessment through drinking water intake

Co-kriging methods

Geostatistics it was widely used in the characterization of groundwater quality and the simulation of the hydrogeological variables (Selmane et al., 2023a; Belkhiri et al., 2020; Richa et al., 2015). Geostatistics consists of variography and kriging. Variography uses semivariograms to characterize and model the spatial variance of data, whereas kriging uses the modeled variance to estimate values between samples (Burgess & Webster, 1980; Cahn et al., 1994).

Semivariograms were first used by G. Matheron in 1963. It was later applied in fields related to spatial data such as ecology, meteorology, geology, etc.

A semivariogram is a graphical representation of the variance of data as a function of the distance between measurement points. Shows the difference in measure and distance between all pairs of sampled locations (Bansal et al., 1993).

It refers to the spatial correlation in observations measured at sample locations. Semivariogram modeling is also used as a prediction tool to estimate the value of a measure at a new location. (Chiles & Delfiner, 2012). The semivariogram is given by the following equation:

$$\gamma(h) = \frac{1}{2N(h)} \sum_{i=1}^{N(h)} [Z_{(x_i)} - Z_{(x_i+h)}]^2 \quad (2)$$

Where γ is the semi variance for N data pairs separated by a distance of h, known as a lag, and Z is the value at positions x_i and $x_i + h$. (Rostami et al., 2020, Selmane et al., 2022a).

Co-kriging is a geostatistical technique generalizing the kriging to multivariate interpolation. It exploits the correlation between the different variables as well as the spatial structure of the data, and also use the slope information in conjunction with the variable itself (Rostami et al., 2020; Chiles & Delfiner, 2012).

Co-Kriging estimator it is a very flexible interpolation method, allow the user to investigate graphs of crosscorrelation and autocorrelation. Co-Kriging estimation is introduced by the following equation:

$$\sum_{l=1}^{v} \sum_{i=1}^{n} \lambda_{il} \lambda_{iv} \gamma(x_i, x_j) - \mu_{uv} = \gamma_{uv}(x_i, x_p) \; where \; j = 1, \dots, n \; and \; u = 1, \dots, v$$

$$with \; \sum_{i=1}^{nl} \lambda_{il} = \begin{cases} 1, & 1 = u \\ 0, & 1 \neq 1u \end{cases} \quad (3)$$

where u and v are the primary and secondary variables, respectively.

For Co-Kriging analysis, the cross-variogram should be determined in prior (Belkhiri et al, 2020). The cross-variogram models between the primary and secondary variables are obtained by fitting with an experimental cross-variogram that is given by:

$$\gamma_{uv}(h) = \frac{1}{2N(h)} \sum_{i=1}^{N(h)} [z_u(x_i) - z_u(x_i + h)][z_v(x_i) - z_v(x_i + h)] \quad (4)$$

Results and discussion

General quality of groundwater in the study area

In this study and based on statistical analyses of 60 samples of 2022 campaign (Table 1), it was observed that 41.7 and 96.7% of the samples exceeded the standard of WHO 2011 for Cl^-, SO_4^{2-}. Nearly 78.3% of the water samples contained concentrations of more than 50 mg/l of nitrates. Conductivity and total hardness exceeded the recommended standard (WHO, 2011) in the majority of the samples studied.

Chloride, nitrate and sodium showed a high coefficient of variation 74.5%, 75.8%, and 53.1 respectively, which indicates a significant spatial variation between minimum and maximum values in the samples and a clear deviation of these parameters from the mean. These variations can be attributed to the influence of pollution. The coefficients of variation for TDS, EC, Mg^{2+}, HCO_3^-, SO_4^{2-} and K^+ were lower indicating that the concentrations of these elements are relatively consistent in the study area. This pattern suggests the influence of water–rock interactions, including the dissolution and precipitation of minerals such as gypsum, halite, anhydrite, and calcite, on the water chemistry.

The principal component PC1 represents 51.9% of the variance of physicochemical parameters and is attributed to a strong correlation with the following parameters EC, TDS, Ca^{2+}, Cl^-, SO_4^{2-}, TH and Na^+ (Fig. 7), indicating the presence of evaporite mineralization. Principal component PC2 takes 15.4% of the variance of water quality and shows a good correlation with T and bicarbonate (Fig. 7) indicates the carbonate precipitation process. The principal component PC3(9.3%) combines pH, NO_3^- and K^+ it indicates the presence of anthropogenic pollution.

Table 1. *Statistical description of the physicochemical results of the 60 samples in 2022 campaign*

Variable	WHO 2011	Min	Max	Mean	CV	% Sample exceeding the WHO standard
T	-	14.8	33.6	18.4	25.7	0
pH	8.5	6.5	8.15	7.5	3.9	0
EC	1500	1035.8	4901.8	2479.9	30.4	93.3
TDS	1000	213	1825.5	962.1	31.15	35
Ca^{2+}	75	104	601.2	255.8	46	100
Mg^{2+}	100	36.4	255.2	96.6	39.8	40
HCO_3^-	300	149.4	427	217.7	25.9	8.3
Cl^-	250	56.8	923	299.3	74.5	41.7
SO_4^{-2}	250	250	1300	629.4	32.2	96.7
TH	500	420	2450	1046.2	41.2	96.7
NO_3^-	50	2	407	127.8	75.8	78.3
Na^+	200	41	379.1	113.8	53.2	5
K^+	12	4.7	16	7.2	29.3	5

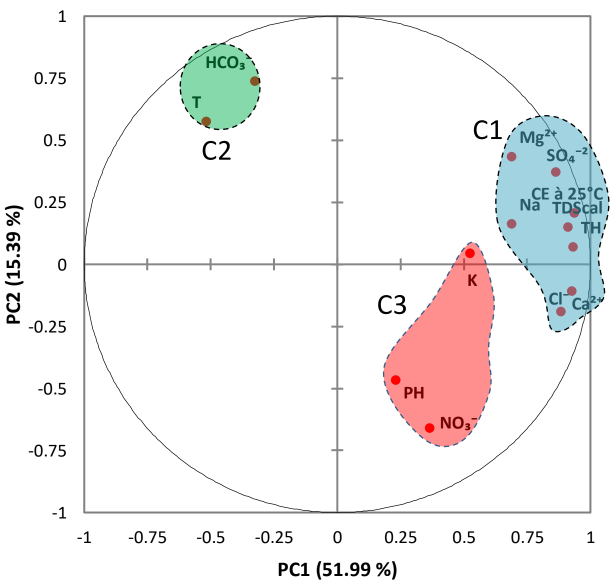

Fig. 7. Plot of Correlation between the principal components and physicochemical parameters using PCA method

Temporal evolution of nitrates

Table 2 shows the evolution of the average nitrate concentration in the groundwater of Bousaada region from 1967 to 2022. All the measurement campaigns have average nitrate concentrations greater than or equal to 50 mg/l at the legal threshold, except the 1967 campaign where the average concentrations are within the authorized standard. It can be seen that nitrate continues to increase reaching a maximum of 127.7 mg/l after being practically maintained at 60 mg/l between 1967 and 1996. We note that most of the samples studied during the 1967 and 1996 measurement campaigns contain concentrations around 50 mg/l, respectively 63 and 58.2%. On the other hand, the samples studied in the years 2018, 2019, and 2022 contain values mostly above 50 mg/l with an increase of more than 60%. Even more intriguing, it was found that 50% of the samples analyzed during the 2022 campaign had readings above 100 mg/l.

These results show that nitrates have been present in the groundwater of the region for decades and have multiplied significantly and alarmingly in recent years.

Table 2. *Statistical description of nitrate concentrations from 1967 to 2022*

Years	1967	1996	2018	2019	2022
Number of samples	61	50	19	29	60
Min	0	11	2	7	02
Max	177	310	120	184	407
Mean	63	58	67.3	73.9	127.7
% low 50	53.2	76	31.6	37.5	21.6
% high 50	46.8	24	63.2	62.5	78.3
% high 100	22.6	12	15.8	31.2	50

Evaluation of nitrate pollution and its health risks

Nitrate pollution index NPI

Figure 8.a presents the classification of groundwater for the samples studied in 2022. According to the NPI value, five types of water have been identified: Very good (< 0), good (0 to 1), moderate status (1 to 2), poor status (2 to 3) and bad status (> 3).

It was reported that only 8.3% of the total samples belonged to the clean categories and 5% of the samples belonged to the Slightly polluted categories, and 16.6% of the samples studied were in the moderately polluted category. On the other hand, 70% of the samples are clearly polluted by nitrates (where it was 8.3% heavily polluted and 61.6% ery heavily polluted).

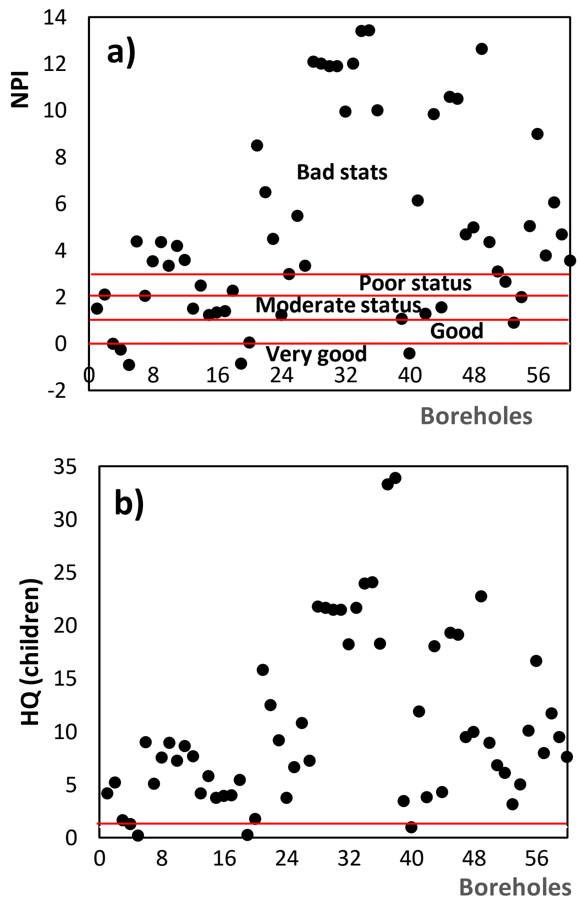

Fig. 8. a) Classification of nitrate pollution levels (NPI) and ; b) health risque from drinking (HQ for children)

In order to examine the variations in the level of pollution by nitrates in groundwater and the factors that influenced them in the region of Bousaada, a spatial distribution map of NPI values was carried out to predict the level of pollution by nitrates using the ordinary kriging method by ArcGIS 10.8 software.

The results of spatial interpolation of the NPI for the samples studied (Fig 9) show that the agricultural perimeter of Maadher and the boreholes close to the wadi of Bousaada are exposed to heavy pollution by nitrates. On the other hand, the level of pollution gradually decreases as it moves away from Oued Bousaada, and the intensity of agriculture was reduced.

The samples located in the high areas and outside the agricultural perimeter are clean and not polluted by nitrates. According to these classifications, this pollution by nitrate may be due to many factors, including intensive agricultural activities, pollution from Wadi Bousaada, and the intensive number of septic tanks in the region.

Human Health Risk Assessment of nitrate

Evaluating the potential impact of a risk on human health is done through the process of HHRA. Groundwater is the only source for agriculture and domestic uses for the residents of the area, so it is important to assess the non-carcinogenic health risk in the study area. An efficient tool for evaluating non-cancer health risks in various age groups in the study area

Figure 8b present the hazard quotient (HQ) for nitrate in all samples and for both age groups adults and children. For the children, all HQ values are above 1 except the boreholes 5, 19 and 40. where indicate that 95% of samples are in the high-risk class. As for the adults, we also observe that boreholes 4, 5, 19, and 40 are less than 1, which is 93.3% of samples in the high-risk class.

Figure 9b shows the spatial interpolation of HQ values for children, using ordinary kriging, Through the spatial distribution results of HQ values, it was determined that the boreholes located in the agricultural perimeter of Maadher and near Wadi Bousaada posed a great threat to the health of the residents. Figure 9 shows the spatial interpolation of HQ values for children, using ordinary kriging, Through the spatial distribution results of HQ values, it was determined that the boreholes located in the agricultural perimeter of Mmaadher and near Wadi Bousaada and Maiter posed a great threat to the health of the residents. As for the rest of the boreholes scattered in the studied area (18, 17, 24, 16, 8, 6, 14, 11, 12, 2, 1, 27, and 3), the risk percentage remains uneven for human health, except for boreholes 4, 5 and 19 in the far west and borehole 40 (Fig 8b), as it contains excelent water qaulity and does not pose a risk to the health of the residents.

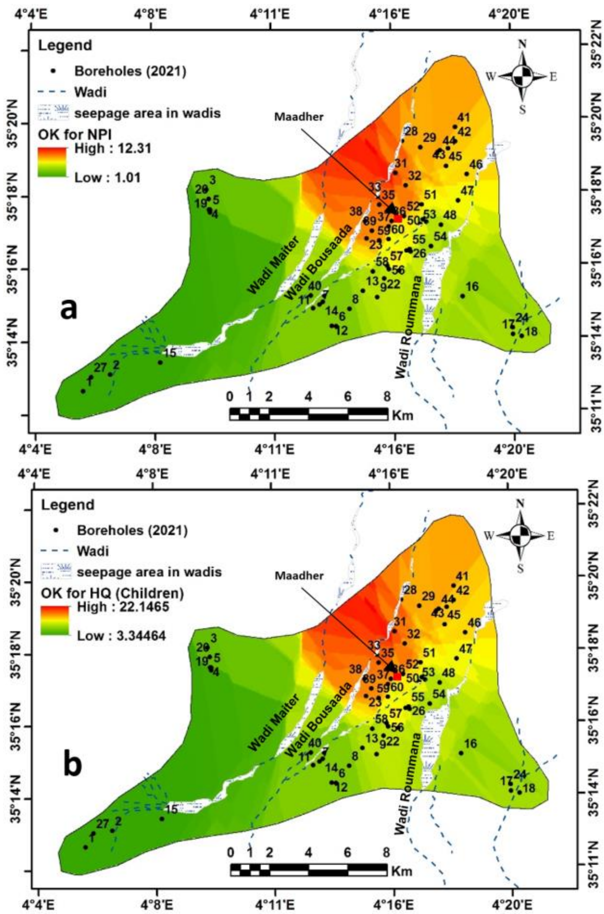

Fig. 9. Spatial interpolation maps of a) NPI and b) HQ of HHRA using the ordinary kriging method

Origin of nitrate

Nitrogen fertilizers contain NO_3^- and Cl^- ions, such as ammonium chloride (NH_4Cl), ammonium nitrate (NH_4NO_3), and others. Some quantities of nitrogen fertilizers are absorbed by crops, and the rest is usually converted to NO_3^- by nitrification and entering the aquifer (Mekala et al., 2017). Since the area is characterized by sandy soil, this process occurs easily and quickly. As a result, it is possible that NO_3^- pollution is related to agricultural practices. In addition to chlorine being associated with agricultural fertilizers, it is also associated with wastewater (Redwan et al., 2020; El Mountassir et al., 2022).

The NO_3^-/Cl^- ratio is used as an index of mixing or biological processes such as nitrification, denitrification, and remineralization, which affects the distribution and behavior of nitrates and chlorides (Li et al. 2010; Djema & Mebrouk, 2022). Usually, chemical fertilizers contain high concentrations of NO_3^- and have a high NO_3^-/Cl^- ratio and wastewater has a high content of Cl^- and a low NO_3^-/Cl^- ratio (Djema & Mebrouk, 2022; Yue et al., 2017). In addition, chlorine can disrupt the activity of nitrate reductase and other enzymes used for the nitrate reduction to nitrogen gas (Rusmana & Nedwell, 2004). Consequently, the nitrate levels in the groundwater may remain elevated, as the denitrification process is slowed down or stopped.

The NO_3^-/Cl^- ratio versus Cl^- concentrations was plotted to determine the sources of nitrate in groundwater. The results show in Figure 10a that samples 26, 29, 30, 37, 39, 41, 42, 43, 44, 46, 47, 48 and 50 have a high Cl^- content, suggesting the source of nitrogen is mainly from the contribution of sewage or animal manure (it's widely used as fertilizer in the study area); These borehles also showed a clear clustering with PC1 in the PCA analysis, and it was also observed that they clustered in the area exposed to the anthrpogenic pollution with nitrate (Fig.9), which confirms this hypothesis. The samples 6, 9, 13, 14, 17, 18, 21, 23, 27, 28, 31, 33, 35, 36, and 38 have a low Cl^- content and a high ratio of NO_3^-/Cl^-, it indicates that agricultural input is the likely source of nitrates in these samples ; Its clear clustering with PC2 was also observed in the principal component analysis (PCA), as well as its clustering in the agricultural perimeter of Maadher (Fig 9), which confirms the agricultural inputs hypothesis. The rest of the samples did not take a clear direction through which the source of nitrates could be identified, because these samples contain weak concentrations of chloride and nitrates. In addition, these wells are located far from population centers and intensive agricultural activities.

The scatter plot of TDS (g/L) versus $(NO_3^-+Cl^-)/HCO_3^-$ (meq/L) was used in this study to identify the anthropogenic inputs to groundwater. These diagrams have been widely used in similar studies for identifying the sources of NO_3^- pollution (Xu et al, 2023; He et al. 2022). The obtained results showed a positive regression between TDS and $(NO_3^-+Cl^-)/HCO_3^-$, with a determination coefficient of 0.4 (Fig.10b), suggesting that the groundwater quality in the study area was seriously affected by anthropogenic inputs (Xu et al., 2023).

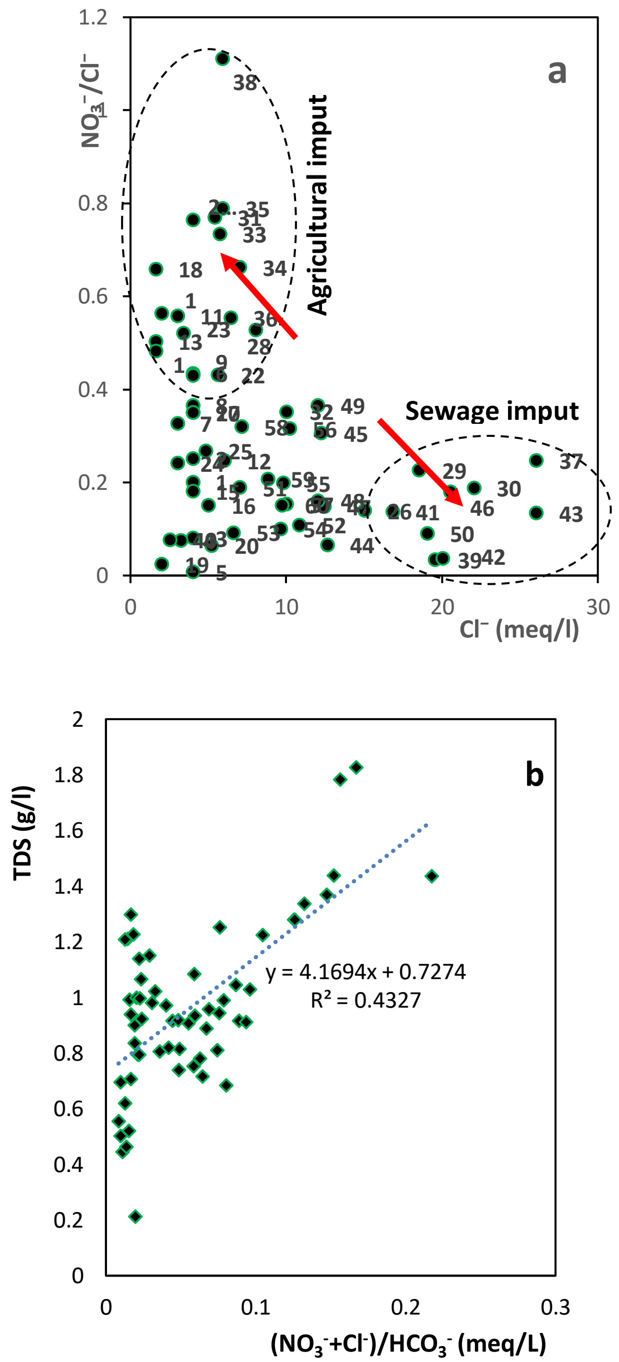

Fig. 10. Nitrate origin and identification (a) bivariate plot of NO_3^-/Cl^- versus Cl^- and (b) TDS versus $(NO_3^-+Cl^-)/HCO_3^-$

Anthropogenic activities are a major factor affecting groundwater pollution by nitrates. Where NO_3^- mainly originates from agricultural activities and household sanitation inputs (Li et al., 2023; Liu et al., 2021; Ren et al., 2022), Cl^- and SO_4^{2-} in groundwater may come from evaporation of gypsum and halite. The anthropogenic activities can also lead to elevated Cl^- and SO_4^{2-} in groundwater (Li et al., 2023).

In Figure 11a, the studied samples are generally characterized by high molar ratios of Cl^-/Na^+ and NO_3^-/Na^+ mainly located near the upper right corner of the 1:1 line, which indicates that the high nitrate in the groundwater of the study area mainly comes from the agricultural activities. At the same time, the relationship between the ratios of NO_3^-/Na^+ and SO_4^{2-}/Na^+ (Fig.11b) showed that industrial activities also influence the chemical properties of groundwater to a certain extent. While ratios suggest possible industrial influence, field investigation found no significant industrial activities, except some small private workshops. On the other hand, there is heavy use of fertilizers such as organic fertilizers (manure and compost), synthetic fertilizers and livestock dung. In addition, high sulfate concentration is due to the water chemical quality that indicates a sodium-sulfate facies. Therefore, agricultural activities are assumed to be the most likely source of nitrate contamination.

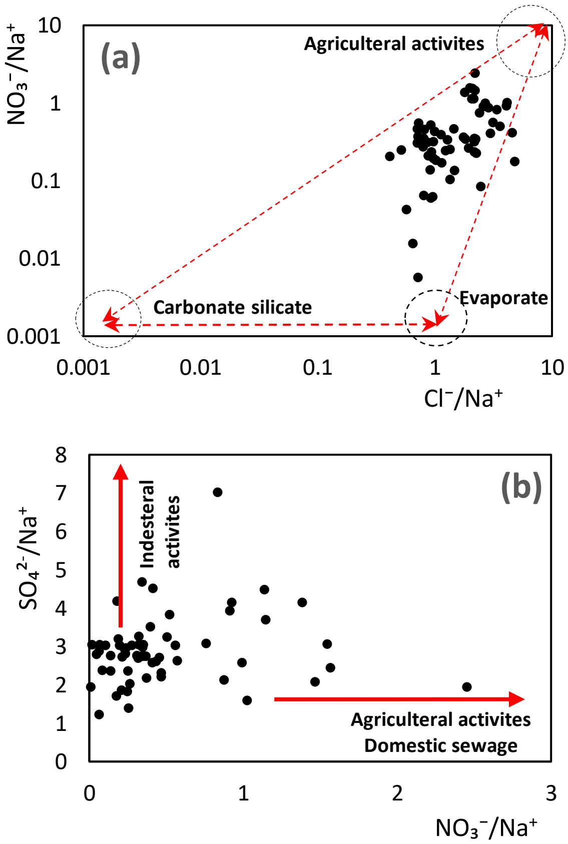

Fig. 11. Plots of (a) Cl^-/Na^+versus NO_3^-/Na^+ and (b) NO_3^-/Na^+ versus SO_4^{2-}/Na^+

Figure 12a shows that HCO_3^- increases when NO_3^- decreases. On the other hand, we note that when nitrate levels increase, chloride levels also increase, especially for samples containing NO_3^- greater than 50 mg/L (Fig. 12b). The remarkable increases in nitrate concentrations are due to evaporation and intrusion of irrigation water to the aquifer. This phase contributes to the dissolving of minerals, fertilizers, and agricultural residues. This leads to decreased bicarbonate in favour of chlorides and nitrates (Li et al., 2023; Traboulsi et al., 2005).

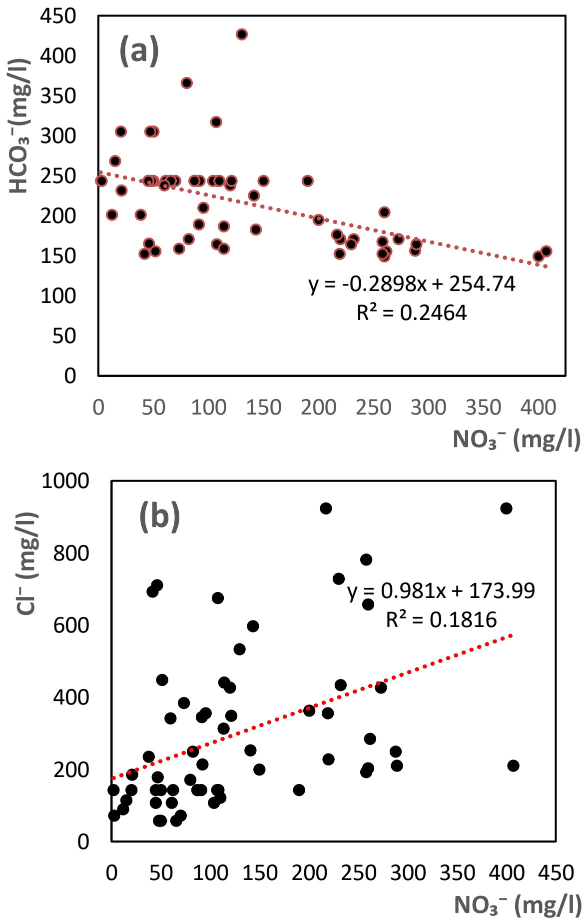

Fig. 12. Plots of (a) nitrate versus bicarbonate and (b) nitrate versus chloride

The effect of physical factors on groundwater pollution with nitrates

The Ordinary Kriging (OK) was applied using spherical models to predict nitrate concentrations without covariates. Then, co-kriging (CK) was applied with covariates. initially several variogram and cross-variogram models (spherical, exponential, and Gaussian) were tested, experimental variograms were calculated for the primary variables and cross-variograms between the primary and secondary variables. and the best-fitting model was selected based on the lowest residual sum of squares and visual agreement with the experimental variograms. The spherical model provided the best fit for most variables and was therefore adopted for both the variogram and cross-variogram structures.

The chloride cncentrations, the number of septic tanks near each sample, the average distance of septic tanks from samples, the distance of samples from wadi Bousaada and land uses used as covariates in the co-kriging interpolation. This covariates were selected based on the field investigations conducted in the study area, and based on the inferred factors that contribute to the nitrate pollution, and based on their statistical correlation with the primary variable.These were observed to be very influential factors in the presence of nitrate at high concentrations in the area.

By comparing Figure 13a with Figure 13b, c, d, e, and f, one can see the effect of these covariables on nitrate concentrations in the studied area. The CK maps with co-variables (Fig.13b, c, d, e, and f) provide some new and accurate locations compared to the OK map. High nitrate values can be observed in the north of the studied area near Wadi Bousaada and the Maadhar area (with intense agricultural activity).

Map 14b shows the effect of chloride concentration on spatial variations of nitrate, where the focus of high nitrate concentrations appeared wider, indicating the common source of chloride and nitrate.

The effect of the number of septic tanks and their distance from the studied samples is clearly evident on the nitrate concentration (Fig.13c and d). The greater the number of pits and the shorter the distance from the studied samples, the stronger and more evident the nitrate pollution.

As for Wadi Bousaada, its effect was clear in Figure 13e, where it appeared that the samples close to the outlets of Wadi Bousaada contain high concentrations of nitrate.

It was noted through Figure 13f that the area of high agricultural activities (Maadher) showed a strong correlation with nitrate distributions. It indicates the direct effect of the use of industrial and animal fertilizers on groundwater pollution with nitrates.

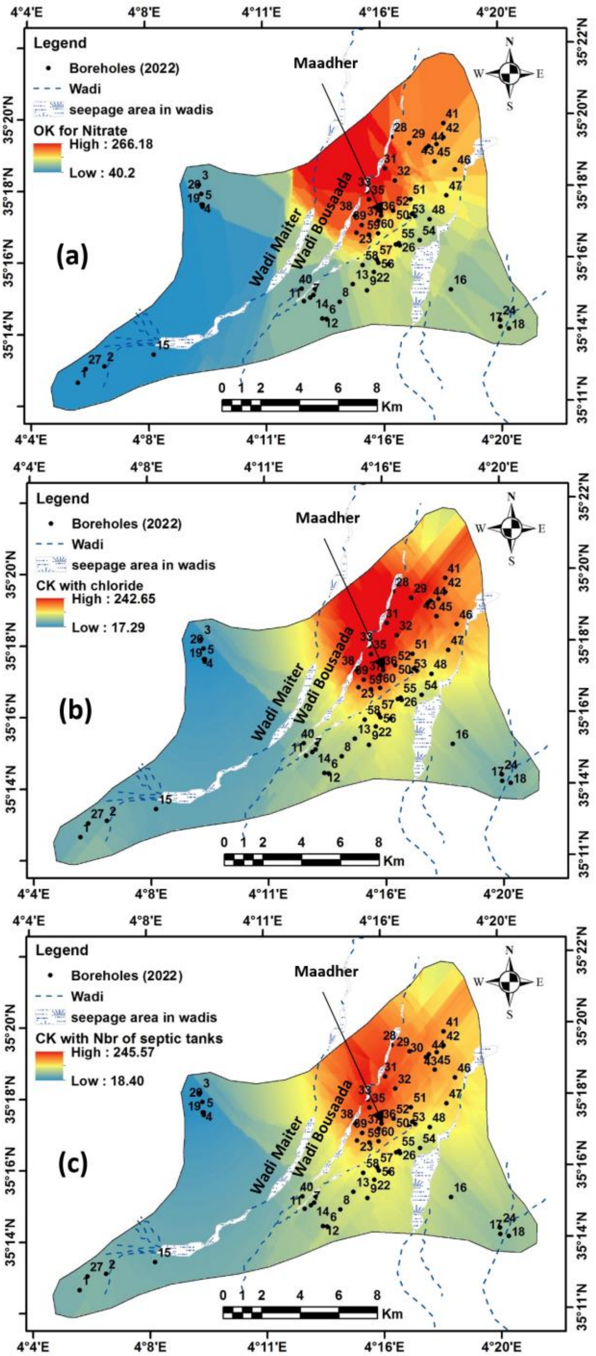

4°4'E
4°8'E
4°11'E
4°16'E
4°20'E
35°22'N
35°20'N
35°18'N
35°16'N
35°14'N
35°11'N
Legend
Boreholes (2022)
Wadi
seepage area in wadis
OK for Nitrate
High : 266.18
Low : 40.2
Maadher
Wadi Maiter
Wadi Bousaada
(a)
0 1 2 4 6 8
Km
Legend
Boreholes (2022)
Wadi
seepage area in wadis
CK with chloride
High : 242.65
Low : 17.29
Maadher
Wadi Maiter
Wadi Bousaada
(b)
0 1 2 4 6 8
Km
Legend
Boreholes (2022)
Wadi
seepage area in wadis
CK with Nbr of septic tanks
High : 245.57
Low : 18.40
Maadher
Wadi Maiter
Wadi Bousaada
(c)
0 1 2 4 6 8
Km
N
S
W
E

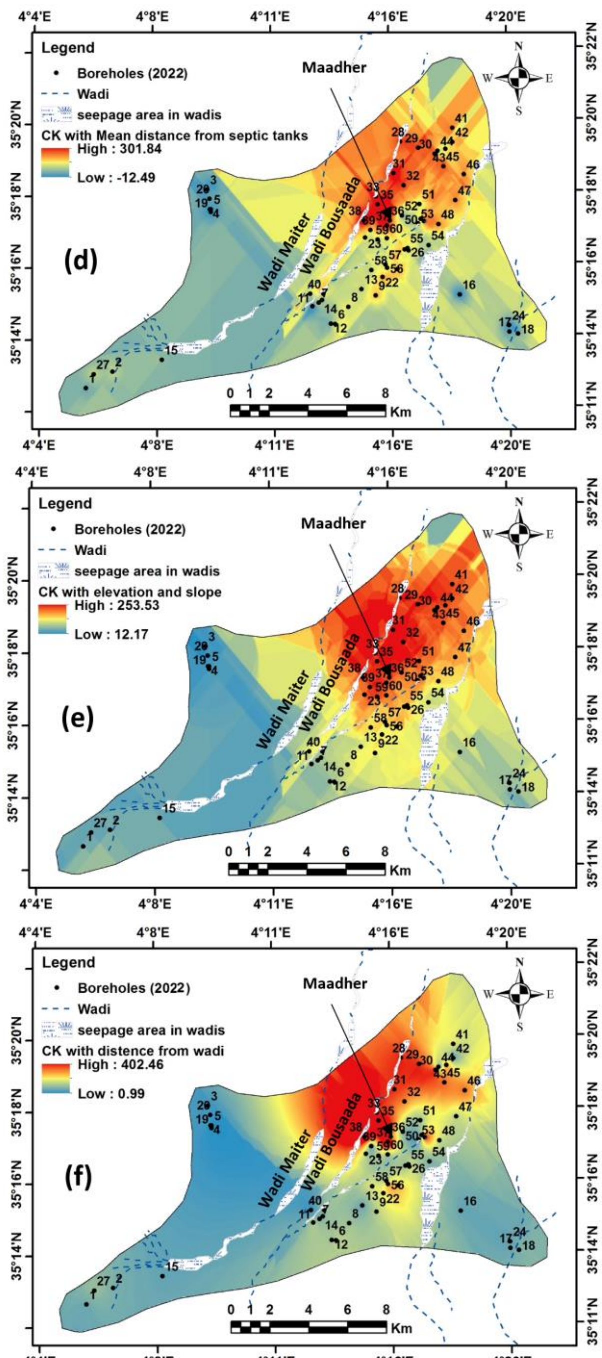

Fig. 13. Spatial prediction map of NO_3^- obtained by (a) Ordinary Kriging (OK), (b) Co-Kriging (CK) with chloride, (c) CK with Nbr of septic tanks, (d) CK with Mean distance from septic tanks, (e) CK with land use and (f) CK with distance from wadi

Conclusion

This study evaluated the hydrogeochemical characteristics, nitrate contamination, spatial distribution, and associated health risks of groundwater in the Bousaada region using physicochemical data from 60 samples collected in 2022 supported by historical datasets from 1967–2019. The results reveal a clear deterioration in groundwater quality, characterized by high salinity and significant nitrate contamination. A large proportion of the samples exceeded drinking water standards, with 41.6% and 96.6% surpassing the limits for Cl^- and SO_4^{2-}, respectively, and 78.3% containing nitrate concentrations above 50 mg/L. The EC and TH were also elevated in most samples, indicating strong mineralization influenced by both natural processes, such as the dissolution and precipitation of geological composition (Gravels, Conglomerates, clays, marls, sandstones, limestones, evaporitic deposits and dolomites), and anthropogenic inputs. The temporal analysis shows a marked increase in nitrate concentrations since 1967, reaching an average of 127.7 mg/L in 2022, with more than half of the samples exceeding 100 mg/L. The NPI Index confirmed severe contamination, with about 70% of groundwater samples classified as polluted, particularly in the agricultural area of Maadher and near Wadi Bousaada. HHRA further indicated that groundwater consumption may pose significant non-carcinogenic risks, as hazard quotient values exceeded the safe threshold for 95% of children and 93.3% of adults. Hydrogeochemical and multivariate statistical analyses revealed that groundwater chemistry is controlled by both natural mineralization processes and anthropogenic activities. ion ratios and bivariate diagrams suggests that agricultural fertilizers, septic tanks, and wastewater discharges are the main contributors to nitrate contamination, while geostatistical modeling demonstrated that co-kriging with environmental covariates improved the spatial prediction of nitrate distribution and highlighted the strong influence of agricultural activities, septic tank density, and proximity to Wadi Bousaada on groundwater pollution with nitrate.

Conflict of Interest: The authors declare no conflict of interest.

Publisher's Note: Serbian Geographical Society stays neutral with regard to jurisdictional claims in published maps and institutional affiliations.

References

Anjana, S.U., & Iqbal, M. (2007). Nitrate accumulation in plants, factors affecting the process, and human health implications. *Agronomy for Sustainable Develepment*, 27 (1), 45-57. DOI:10.1051/agro:2006021

Askri, H., Belmecheri, A., Benrabah, B., Boudjema, A., Boumendjel, K., Daoudi, M., & Terkmani, M. (1995). Geology of Algeria. In Well Evaluation Conference Algeria, 1-93.

Abdesselam, S., Halitim, A., Jan, A., Trolard, F., & Bourrié, G. (2013). Anthropogenic contamination of groundwater with nitrate in arid region: case study of southern Hodna (Algeria). *Environmental Earth Sciences,* 70(5), 2129-2141. https://doi 10.1007/s12665-012-1834-5

Adimalla, N., Li, P., & Qian, H. (2018). Evaluation of groundwater contamination for fluoride and nitrate in semi-arid region of Nirmal Province, South India: a special emphasis on human health risk assessment (HHRA). *Human and ecological risk assessment: An International Journal*, 25(5), 1107-1124. https://doi.org/10.1080/10807039.2018.1460579

Adimalla, N., Qian, H., & Nandan, M. J. (2020). Groundwater chemistry integrating the pollution index of groundwater and evaluation of potential human health risk: a case study from hard rock terrain of south India. *Ecotoxicology and Environmental Safety*, 206, Article 111217. https://doi.org/10.1016/j.ecoenv.2020.111217

Azhdarpoor, A., Radfard, M., Pakdel, M., Abbasnia, A., Badeenezhad, A., Mohammadi, A. A., & Yousefi, M. (2019). Assessing fluoride and nitrate contaminants in drinking water resource and their health risk assessment in a semiarid region of southwest Iran. *Desalination and Water Treat*, 149, 43-51. https://doi.org/10.5004/dwt.2019.23865.

Akhtar, M., Hussain, F., Ashraf, M. Y., Qureshi, T., M., Akhter, J., & Awan A. R. (2012). Influence of Salinity on Nitrogen Transformations in Soil. *Communications in Soil Science and Plant Analysis*, 43, 1674-1683. https://doi.org/10.1080/00103624.2012.681738

Bahrami, M., Zarei, A. R., & Rostami, F. (2020). Temporal and spatial assessment of groundwater contamination with nitrate by nitrate pollution index (NPI) and GIS (case study: Fasarud Plain, southern Iran). *Environmental Geochemistry and Health*, 42(10), 3119-3130. https://doi.org/10.1007/s10653-020-00546-x

Burgess, T. M., & Webster, R. (1980). Optimal interpolation and isarithmic mapping of soil properties: II block kriging. *Journal of Soil Science*, 31(2), 333-341. https://doi.org/10.1111/j.1365-2389.1980.tb02085.x

Belkhiri, L., Tiri, A., & Mouni, L. (2020). Spatial distribution of the groundwater quality using kriging and Co-kriging interpolations. *Groundwater for Sustainable Development*, 11, Article 100473. https://doi.org/10.1016/j.gsd.2020.100473

Bansal, S., Merrill, M. R., & Deans, H. A. (1993). Application of the semivariogram to MRI data: a useful approach for the characterization of natural porous rocks. *Applied Magnetic Resonance*, 4, 241-259. https://doi.org/10.1007/BF03162500

Boudjemline, F., & Semar, A. (2018). Assessment and mapping of desertification sensitivity with MEDALUS model and GIS–Case study: basin of Hodna, Algeria. *Journal of water and land development*, 36(1), 17-26. DOI: 10.2478/jwld-2018-0002

Benazzouz, Mohamed, T. (1994). Étude des interactions relief-migrations éoliennes de sable dans la région de M'Doukal (Algérie). In: Méditerranée, 80(3-4). Géographie physique de l'Algérie orientale. pp. 51-58. https://doi.org/10.3406/medit.1994.2858

Benchetrif, M. (1956). Les sols d'Algérie Revue de Géographie Alpine Année, 44-4. pp. 749-761. https://doi.org/10.3406/rga.1956.1790

Boyadgifv, T. G. (1975). FAO Soil Expert Hodna Soil Map. (in French)

Chiles, J. P., & Delfiner, P. (2012). *Geostatistics: modeling spatial uncertainty* (Vol. 713). John Wiley & Sons.

Cahn, M. D., Hummel, J. W., & Brouer, B. H. (1994). Spatial analysis of soil fertility for site-specific crop management. *Soil Science Society of America Journal*, *58*(4), 1240-1248. https://doi.org/10.2136/sssaj1994.03615995005800040035x

Djema, M., & Mebrouk, N. (2022). Groundwater quality and nitrate pollution in the Nador plain, Algeria. *Environmental Earth Sciences*, *81*(18), Article 460.https://doi.org/10.1007/s12665-022-10557-9

Derekov, A. M. (1973). Hydrological studies in the Chott El Hodna basin. Technical report, FAO.

El Mountassir, O., Bahir, M., Ouazar, D., Chehbouni, A., & Carreira, P. M. (2022). Temporal and spatial assessment of groundwater contamination with nitrate using nitrate pollution index (NPI), groundwater pollution index (GPI), and GIS (case study: Essaouira basin, Morocco). *Environmental Science and Pollution Research*, 29, 17132–17149. https://doi.org/10.1007/s11356-021-16922-8

Guiraud, R. (1970). Quaternary morphogenesis of the Hodna region (Northern Algeria) (in French). In Annals of Geography. Persée-Portal of scientific journals in SHS, 79(433), 367-374.

Guiraud, R. (1973). The main features of the Hodna Chott basin Hydrogeology, Northern Algeria (in French). *Publi. servi. Géol*. 39, 159–170.

Guo, J., Yongxue, Z., Guo, H., & Min, W. (2021). Saline and alkaline stresses alter soil properties and composition and structure of gene-based nitrifier and denitrifier communities in a calcareous desert soil, Guo et al. BMC *Microbiology,* 21, Article 246. https://doi.org/10.1186/s12866-021-02313-z

Gangwar, R. K., Marianna, M., Bresilla, B., Zain, M., Weldmichael, T.G., Demeter, I., Táncsics, A., Cserháti, M., & Szegi, T. A. (2022). Effects of land uses and soil types on microbial activity and community structure. *International Agrophysics*, 36(4), 323-336. https://doi: 10.31545/intagr/155096

He, S., Li, P., Su, F., Wang, D., & Ren, X. (2022). Identification and apportionment of shallow groundwater nitrate pollution in Weining Plain, northwest China, using hydrochemical indices, nitrate stable isotopes, and the new Bayesian stable isotope mixing model (MixSIAR). *Environmental Pollution*, 298, Article 118852. doi:10.1016/j.envpol.2022.118852.

Kebiche, M. (1994). Le bassin versant du Hodna (Algérie): Ressources en eau et possibilités d'aménagement. In: *Travaux de l'Institut Géographique de Reims*, n°85-86. *Etudes algériennes*. pp. 25-34. https://doi.org/10.3406/tigr.1994.1298

Kamarehie, B., Jafari, A., Zarei, A., Fakhri, Y., Ghaderpoori, M., & Alinejad, A. (2019). Non-carcinogenic health risk assessment of nitrate in bottled drinking waters sold in Iranian markets: a Monte Carlo simulation. *Accrédit. Qual. Assur*, 24, 417–426. https://doi.org/10.1007/s00769-019-01397-5

Kaiser, H.F. (1960). The application of electronic computers to factor analysis. *Educ Psychol Meas*, 20(1), 141–151.

Liu, J.T., Peng, Y.M., Li, C.S., Gao, Z.J., & Chen, S.J. (2021). Characterization of the hydrochemistry of water resources of the Weibei Plain, Northern China, as well as an assessment of the risk of high groundwater nitrate levels to human health. *Environmental Pollution*, 268, Article 115947. https://doi.org/10.1016/j.envpol.2020.115947

Li, D., Zhai, Y., Lei, Y., Li, J., Teng, Y., Lu, H., Yang, J. (2021). Spatiotemporal evolution of groundwater nitrate nitrogen levels and potential human health risks in the Songnen Plain, Northeast China. *Ecotoxicology Environmental Safety*, 208, Article 111524. 111524 doi:10.1016/j. ecoenv.2020.111524.

Li, X., Huang, X., Zhang, Y. (2021). Spatio-temporal analysis of groundwater chemistry, quality and potential human health risks in the Pinggu basin of North China Plain: evidence from high-resolution monitoring dataset of 2015-2017. *Science of the Total Environment*, 800, 149568. https://doi.org/10.1016/j.scitotenv.2021.149568

Li, Z., Yang, Q., Xie, C., & Lu, X. (2023). Source identification and health risks of nitrate contamination in shallow groundwater: a case study in Subei Lake basin. *Environmental Science and Pollution Research*, *30*(5), 13660-13670. https://doi.org/10.1007/s11356-022-23129-y

Li, S.L., Liu, C.Q., Li, J., Liu, X., Chetelat, B., Wang, B., & Wang, F. (2010). Assessment of the sources of nitrate in the changjiang river, china using a nitrogen and oxygen isotopic approach. *Environmental Science and Technology*, 44(5), 1573–1578. https:// doi. org/ 10. 1021/ es902 670n

Matheron, G., (1963). Principles of geostatistics. *Economic Geology*, 58, 1246–1266. https://doi.org/10.2113/gsecongeo.58.8.1246.

Mekala, C., Gaonkar, O., & Nambi, I.M. (2017). Understanding nitrogen and carbon biogeotransformations and transport dynamics in saturated soil columns. *Geoderma,* 285, 185–194. https:// doi. org/10. 1016/j. geode rma. 2016. 10. 004

Maurice, J., & Jean, N. (1977). Deux thèses sur la géologie et l'hydrogéologie du Bassin du Hodna et de ses bordures (Algérie). In: Méditerranée, deuxième série, tome 29, 2-. pp. 103-105. www.persee.fr/doc/medit_0025-8296_1977_num_29_2_1734

Nannipieri, P., Ascher, J., Ceccherini, M. T., Landi, L., Pietramellara, G., & Renella, G. (2003). Microbial diversity and soil functions. *European Journal of Soil Science*, 54, 655–670. https://doi: 10.1046/j.1365-2389.2003.00556.x

Obeidat, M., Edu, vie, Awawdeh, M., Al-Rub, F. A., & Al-Ajlouni, A. (2012). An Innovative Nitrate Pollution Index and Multivariate Statistical Investigations of Groundwater Chemical Quality of Umm Rijam Aquifer (B4), North Yarmouk River Basin, Jordan. *Water Quality Monitoring and Assessment*, 169.

Panneerselvam, B., Muniraj, K., Thomas, M., & Ravichandran, N. (2021). GIS-based legitimatic evaluation of groundwater's health risk and irrigation susceptibility using water quality index, pollution index, and irrigation indexe in semiarid region. In Groundwater resources development and planning in the semi-arid region (pp. 239-268). Springer, Cham. https://doi.org/10.1007/978-3-030-68124-1_13

Park, M.H., Chae-Hong, P., Sim, Y.B., & Hwang, S.J. (2020). Response of Scenedesmus quadricauda (Chlorophyceae) to Salt Stress Considering Nutrient Enrichment and Intracellular Proline Accumulation. *International Journal of Environmental Research and Public Health,* 17(10), Article 3624. https://www.mdpi.com/1660-4601/17/10/3624

Reddy, S., Sunitha, V., & Suvarna, B. (2022). Groundwater quality and its potential health impacts nearby inactive mines using PIG and geospatial technology, Southwestern part of Cuddapah basin, Andhra Pradesh, South India. *Groundwater for Sustainable Development,* 17, Article 100742. https://doi.org/10.1016/j.gsd.2022.100742

Radfard, M., Gholizadeh, A., Azhdarpoor, A., Badeenezhad, A., Mohammadi, A.A., & Yousefi, M. (2019). Health risk assessment to fluoride and nitrate in drinking water of rural residents living in the Bardaskan city, arid region, southeastern Iran. Desalination and Water Treatment, 145, 249–256. https://doi.org/10.5004/dwt.2019.23651

Richa, A., Douaoui, A., Bettahar, N., Qiang, Z., & Mailhol, J. C. (2015). Assessment and modeling the influence of nitrogen input in the soil on groundwater nitrate pollution: plain of upper-cheliff (north Algeria). *Global Nest Journal*, *17*(4), 744-755.

Redwan, M., Moneim, A.A.A., Mohammed, N.E., & Masoud, A.M. (2020). Sources and health risk assessments of nitrate in groundwater, West of Tahta area, Sohag, Egypt. *Episodes Jourlan of International Geoscience*, 43(2), 751-760. https:// doi.org/ 10. 18814/ epiiu gs/ 2020/ 020048

Ren, K., Pan, X., Yuan, D., Zeng, J., Liang, J., & Peng, C. (2022). Nitrate sources and nitrogen dynamics in a karst aquifer with mixed nitrogen inputs (Southwest China): Revealed by multiple stable isotopic and hydro-chemical proxies. *Water Research*, 210, Article 118000. https://doi.org/10.1016/j.watres.2021.118000.

Rostami, A. A., Karimi, V., Khatibi, R., & Pradhan, B. (2020). An investigation into seasonal variations of groundwater nitrate by spatial modelling strategies at two levels by kriging and co-kriging models. *Journal of environmental management*, *270*, 110843. https://doi.org/10.1016/j.jenvman.2020.110843

Rusmana, I., & Nedwell, D.B. (2004). Use of chlorate as a selective inhibitor to distinguish membrane-bound nitrate reductase (Nar) and periplasmic nitrate reductase (Nap) of dissimilative nitrate-reducing bacteria in sediment. *FEMS Microbiology Ecology*, 48 379–386. https://doi.org/10.1016/j.femsec.2004.02.010

Roy, S., Speed, C., Bennie, J., Swift, R., & Wallace, P. (2007). Identifying the significant factors that influence temporal and spatial trends in nitrate concentrations in the Dorset and Hampshire Basin Chalk aquifer of Southern England. *Quarterly Journal of Engineering Geology and Hydrogeology,* 40, 377–392. https://doi.org/10.1144/1470-9236/07-025

Rahmati, O., Samani, A.N., Mahmoodi, N., & Mahdavi, M. (2015). Assessment of the contribution of N-fertilizers to nitrate pollution of groundwater in Western Iran (Case Study: Ghorveh-Dehgelan Aquifer). *Water Qual Expo Health*, 7(2), 143–151. https://doi.org/10.1007/s12403-014-0135-5.

Selmane, T., Dougha, M., Djerbouai, S., Djemiat, D., & Lemouari, N. (2023a). Groundwater quality evaluation based on water quality indices (WQI) using GIS: Maadher plain of Hodna, Northern Algeria. *Environmental Science and Pollution Research*, *30*(11), 30087-30106. https://doi.org/10.1007/s11356-022-24338-1

Selmane, T., Dougha, M., Hasbaia, M., Ferhati, A., & Redjem, A. (2022b). Hydrogeochemical processes and multivariate analysis for groundwater quality in the arid Maadher region of Hodna, northern Algeria. *Acta Geochimica*, *41*(5), 893-909. https://doi.org/10.1007/s11631-022-00553-y

Selmane, T. (2023). Groundwater Quality and Origin of Nitrates in the El Maadher Region of Bousaada, Doctoral Thesis, Mohamed Boudiaf University - M'sila.

Stelzer, R.S., Drover, D.R., Eggert, S.L., & Muldoon, M.A. (2011). Nitrate retention in a sand plains stream and the importance of groundwater discharge. *Biogeochemistry,* 103 (1–3), 91–107. https://doi.org/10.1007/s10533-010-9449-y

Shams, M., Nodehi, R.N., Alimohammadi, M., & Mahvi, A.H. (2009). A survey of nitrate and fluoride in water distribution networks of Tabas. Iran. *World Applied Science Journal*, 7(12), 1516–1520. http://www.idosi.org/wasj/wasj7(12)/9.pdf

Trabelsi, R., Zaïri, M., Smida, H., & Dhia, H. B. (2005). Salinisation des nappes côtières: cas de la nappe nord du Sahel de Sfax, Tunisie. *Comptes Rendus Geoscience*, *337*(5), 515-524. https://doi.org/10.1016/j.crte.2005.01.010

Wu, J., Lu, J., Wen, X., Zhang, Z., & Lin, Y. (2019). Severe nitrate pollution and health risks of coastal aquifer simultaneously influenced by saltwater intrusion and intensive anthropogenic activities. *Arch. Environ. Contam. Toxicol*, 77(1), 1–9. https://doi.org/10.1007/s00244-019-00636-7

Wilde F.D. (2010). Water-quality sampling by the US Geological Survey: standard protocols and procedures. US Geological Survey Fact Sheet. 312(2). https://doi.org/10.3133/fs20103121

WHO. (2011). Guidelines for drinking-water quality. WHO Ed. Retrieved from https://iris.who.int/bitstream/handle/10665/204411/9789241547611_eng.pdf

Xu, D., Li, P., Chen, X., Yang, S., Zhang, P., & Guo, F. (2023). Major ion hydrogeochemistry and health risk of groundwater nitrate in selected rural areas of the Guanzhong Basin, China. *Human and Ecological Risk Assessment: An International Journal*, *29*(3-4), 701-727. https://doi.org/10.1080/10807039.2022.2164246

Xin, J., Wang, Y., Shen, Z., Liu, Y., Wang, H., & Zheng, X. (2021). Critical review of measures and decision support tools for groundwater nitrate management: a surface-to- groundwater profile perspective. J. Hydrol. 598. https://doi.org/10.1016/j. jhydrol.2021.126386.

Yue, F.J., Li, S.L., Liu, C.Q., Zhaoet, Z.Q., & Ding, H. (2017). Tracing nitrate sources with dual isotopes and long term monitoring of nitrogen species in the Yellow River China. *Scientific Report*, 7, Article 8537. https:// doi. org/ 10.1038/ s41598- 017- 08756-7

Yousefi, M., Ghoochani, M., &, Mahvi, A.H. (2018). Health risk assessment to fluoride in drinking water of rural residents living in the Poldasht city, Northwest of Iran. *Ecotoxicol Environ Saf*. 148, 426–430. DOI: 10.1016/j.ecoenv.2017.10.057

Zhang, Y., Wu, J., Xu, B. (2018). Human health risk assessment of groundwater nitrogen pollution in Jinghui canal irrigation area of the loess region, northwest China. *Environmental Earth Sciences*, 77(7), 1-12. https://doi.org/10.1007/s12665-018-7456-9